OPEN ACCESS
CellPress

Cell Reports
Report

Single-Cell Imaging of Caspase-1 Dynamics Reveals an All-or-None Inflammasome Signaling Response

Ting Liu,[1] Yoshifumi Yamaguchi,[1,2,*] Yoshitaka Shirasaki,[3] Koichi Shikada,[1] Mai Yamagishi,[3] Katsuaki Hoshino,[4,5,6] Tsuneyasu Kaisho,[5,6,12] Kiwamu Takemoto,[2,7] Toshihiko Suzuki,[8] Erina Kuranaga,[9] Osamu Ohara,[3,10] and Masayuki Miura[1,11,*]

[1]Department of Genetics, Graduate School of Pharmaceutical Sciences, The University of Tokyo, Bunkyo-ku, Tokyo 113-0033, Japan
[2]PRESTO, Japan Science and Technology Agency, Chiyoda-ku, Tokyo 102-0076, Japan
[3]Laboratory for Integrative Genomics, RIKEN Center for Integrative Medical Sciences (IMS-RCAI), Yokohama, Kanagawa 230-0045, Japan
[4]Department of Immunology, Faculty of Medicine, Kagawa University, Kita-gun, Kagawa 761-0793, Japan
[5]Laboratory for Immune Regulation, World Premier International Research Center Initiative Immunology Frontier Research Center, Osaka University, Suita, Osaka 565-0861, Japan
[6]Laboratory for Host Defense, RIKEN Research Center for Allergy and Immunology, Yokohama, Kanagawa 230-0045, Japan
[7]Department of Physiology, Graduate School of Medicine, Yokohama City University, Yokohama, Kanagawa 236-0004, Japan
[8]Department of Molecular Bacteriology and Immunology, Graduate School of Medicine, University of the Ryukyus, Nakagami-gun, Okinawa 903-0125, Japan
[9]Laboratory for Histogenetic Dynamics, RIKEN Center for Developmental Biology, Chuo-ku, Kobe 650-0047, Japan
[10]Department of Human Genome Research, Kazusa DNA Research Institute, Kisarazu, Chiba 292-0818, Japan
[11]CREST, Japan Science and Technology Agency, Chiyoda-ku, Tokyo 102-0076, Japan
[12]Present address: Department of Immunology, Institute of Advanced Medicine, Wakayama Medical University, 811-1 Kimiidera, Wakayama, Wakayama 641-8509, Japan
*Correspondence: bunbun@mol.f.u-tokyo.ac.jp (Y.Y.), miura@mol.f.u-tokyo.ac.jp (M.M.)
http://dx.doi.org/10.1016/j.celrep.2014.07.012

SUMMARY

Inflammasome-mediated caspase-1 activation is involved in cell death and the secretion of the proinflammatory cytokine interleukin-1β (IL-1β). Although the dynamics of caspase-1 activation, IL-1β secretion, and cell death have been examined with bulk assays in population-level studies, they remain poorly understood at the single-cell level. In this study, we conducted single-cell imaging using a genetic fluorescence resonance energy transfer sensor that detects caspase-1 activation. We determined that caspase-1 exhibits all-or-none (digital) activation at the single-cell level, with similar activation kinetics irrespective of the type of inflammasome or the intensity of the stimulus. Real-time concurrent detection of caspase-1 activation and IL-1β release demonstrated that dead macrophages containing activated caspase-1 release a local burst of IL-1β in a digital manner, which identified these macrophages as the main source of IL-1β within cell populations. Our results highlight the value of single-cell analysis in enhancing understanding of the inflammasome system and chronic inflammatory diseases.

INTRODUCTION

Macrophages (MΦs) play crucial roles in homeostasis by clearing dead cells and connecting innate immunity with adaptive immunity (Mosser and Edwards, 2008). When MΦs detect pathogen-associated molecular patterns (PAMPs) derived from infection or damage-associated molecular patterns (DAMPs) originating from injured tissues, they secrete various types of cytokines to induce inflammation or tissue repair. Interleukin-1β (IL-1β) is a key cytokine that evokes an inflammatory response, and its secretion is mainly regulated by caspase-1, a member of the cysteine-protease family of caspases (Denes et al., 2012).

Caspase-1 is synthesized as an inactive zymogen and then activated via proteolytic cleavage, a process regulated by intracellular multiprotein complexes called inflammasomes (Martinon et al., 2002; Rathinam et al., 2012); the inflammasomes detect PAMPs and DAMPs by using distinct intracellular pattern-recognition receptors such as NLRP3 (Nod-like receptor family, pyrin domain containing 3), NLRC4 (Nod-like receptor family, CARD domain containing 4), and AIM2 (absent in melanoma 2) (Martinon et al., 2002; Rathinam et al., 2012). When PAMPs or DAMPs are detected, procaspase-1 is recruited directly through interactions between the pattern-recognition receptors and procaspase-1 or indirectly through adaptor proteins such as ASC (apoptosis-associated speck-like protein containing CARD) (Schroder and Tschopp, 2010). The recruited procaspase-1 is activated through autoproteolytic cleavage mediated by proximity-induced multimerization. In addition to regulating proinflammatory cytokines, caspase-1 activation has been shown to cause cell death (Miura et al., 1993). In certain cases, caspase-1 is necessary for the execution of necrotic inflammatory cell death, called pyroptosis, in MΦs in response to intracellular bacterial infection (Fink and Cookson, 2005; Miao et al., 2010). However, in other cases, although caspase-1 is activated in response to various PAMPs or DAMPs, deleting or inhibiting caspase-1 is

insufficient for preventing cell death (Broz et al., 2010; Pierini et al., 2012).

Given the aforementioned studies, the activation of most inflammasomes is considered to typically converge on caspase-1 activation, which couples the secretion of the proinflammatory cytokine IL-1β and cell death. However, most of the information on inflammasomes and caspase-1 has been obtained from population-level studies conducted using bulk assays such as western blotting and ELISA, mainly because of technical limitations and because of the unique characteristics of caspase-1 such as rapid secretion after activation and rapid inactivation (Keller et al., 2008; Walsh et al., 2011). Emerging evidence suggests that population data do not faithfully reflect how single cells respond to stimuli (Tay et al., 2010). Thus, the mechanism through which individual cells activate caspase-1 by means of distinct inflammasomes and secrete IL-1β in response to inflammatory stimuli remains unclear. Determining signaling dynamics at the single-cell level not only expands the general understanding of how biological systems work but also complements in vivo studies that examine cells residing in complex contexts (Tay et al., 2010). Single-cell measurement of caspase-1 activity at high spatiotemporal resolution is required to fully understand the dynamics of caspase-1 activation and the direct relationship between caspase-1 activation and its associated outcomes, IL-1β secretion and cell death.

To monitor caspase-1 activity at the single-cell level, we developed SCAT1, a genetically encoded fluorescent sensor for detecting caspase-1 activation based on fluorescence resonance energy transfer (FRET). Using peritoneal MΦs (PMΦs) obtained from transgenic mice expressing SCAT1, we determined that caspase-1 is activated in a digital manner at the single-cell level in response to various types of inflammasomes. Interestingly, the kinetics of caspase-1 activation was similar regardless of the strength and type of stimuli. Moreover, by combining the SCAT1 system and a newly developed technique to measure protein secretion at single-cell resolution, we identified dying MΦs that contained activated caspase-1 as the source of secreted IL-1β in PMΦ populations.

RESULTS

Real-Time Detection of Caspase-1 Activation through the NLRP3 Inflammasome with SCAT1, a Genetically Encoded Probe Developed for Monitoring Caspase-1 Activation

Probes based on FRET technology can provide critical information on the dynamics and activities of endogenous enzymes in living cells (Aoki et al., 2013). We previously generated a genetically encoded probe called SCAT3 (sensor for caspase-3 activation based on FRET) and monitored apoptotic caspase-3 activation in vitro and in vivo (Kuranaga et al., 2011; Nakajima et al., 2011; Takemoto et al., 2003, 2007; Yamaguchi et al., 2011). SCAT comprises 2 fluorescent proteins—enhanced cyan fluorescent protein (ECFP) and Venus—that are connected by a linker sequence that contains caspase cleavage sites (Figure 1A). Upon caspase activation, the linker is cleaved and the FRET between ECFP and Venus is disrupted, which can be detected in real time with fluorescence microscopy. To detect real-time activation of caspase-1, we constructed SCAT1 containing YVAD (a consensus peptide sequence preferentially cleaved by caspase-1) in its linker sequence instead of the DEVD sequence present in SCAT3 (Figure 1A).

The results of in vitro cleavage assays demonstrated that SCAT1 was preferentially cleaved by activated human caspase-1 (Figure S1A). Notably, SCAT1 was barely processed by activated human caspase-4 and caspase-5, which represent potential functional orthologs of murine caspase-11. The specificity of SCAT1 cleavage upon caspase-1 activation was also confirmed in living cells with the caspase-1-specific inhibitor z-YVAD-fmk or by genetic deletion of caspase-1/11 (Figure S1B; see below for a detailed explanation). We generated a gene-targeting mouse line in which the CAG-promoter-loxP-STOP-loxP-SCAT1 gene cassette was knocked into the Rosa26 locus. In this knockin mouse line, SCAT1 expression depended on Cre recombinase expression (Figure S1C); by mating these mice with mice that ubiquitously expressed Cre, we generated mice that expressed SCAT1 in all tissues. We obtained peritoneal MΦs (PMΦs) expressing SCAT1 from these mice. The possibility that overexpressed SCAT1, an exogenous substrate of caspase-1, might prevent the endogenous function of caspase-1 was excluded by our observation that IL-1β secretion and caspase-1 cleavage occurred similarly in PMΦs derived from $SCAT1^{-}$ (wild-type) and $SCAT1^{+}$ mice after inflammasome-activation stimulated with lipopolysaccharide (LPS) + ATP or poly(dA:dT) (Figures S1D and S1E).

Various pathogenic, endogenous, and environmental stimuli can activate the NLRP3 inflammasome after priming with LPS or other Toll-like receptor ligands (Latz et al., 2013). We examined whether SCAT1 can enable real-time detection of caspase-1 activation induced by canonical activators of the NLRP3 inflammasome at the single-cell level. PMΦs collected from SCAT1 knockin mice were stimulated with an environmental danger signal (silica crystals) after LPS priming and were observed continuously under a confocal microscope to monitor the time course of changes in SCAT1 (Venus and ECFP) intensities. The SCAT1 Venus/ECFP (V/C) ratio decreased rapidly and dramatically (Figures 1B and 1C; Movie S1) in some of the cells after stimulation, indicating that caspase-1 was activated; the time of caspase-1 activation varied among cells (Figures S2A and S2B). Moreover, adding the caspase-1-specific inhibitor z-YVAD-fmk abolished the dramatic reduction in the SCAT1 V/C ratio and the cleavage of SCAT1 (Figures 1B, 1C, S1B, S2A, and S2B; Movie S1), indicating that SCAT1 accurately detected caspase-1 activation. We also confirmed that apoptotic caspases were not activated in PMΦs stimulated with LPS + silica; SCAT3, the indicator of caspase-3 activation, did not detect apoptotic activation of caspases in these PMΦs (Figure S2C).

Time-lapse imaging showed that SCAT1 fluorescence disappeared after caspase-1 activation, but the fluorescence was lost even when caspase-1 activation was prevented by its inhibitor (Figure 1B). This loss of fluorescence indicated cell death accompanying membrane rupture because it coincided with the cells becoming positive for TO-PRO-3 or propidium iodide staining (Figure 1D; Movie S1). These data indicated that SCAT1 can faithfully detect NLRP3 inflammasome-induced activation of caspase-1 and subsequent cell death in real time at the single-cell level. Interestingly, the dynamics of SCAT1 V/C ratios

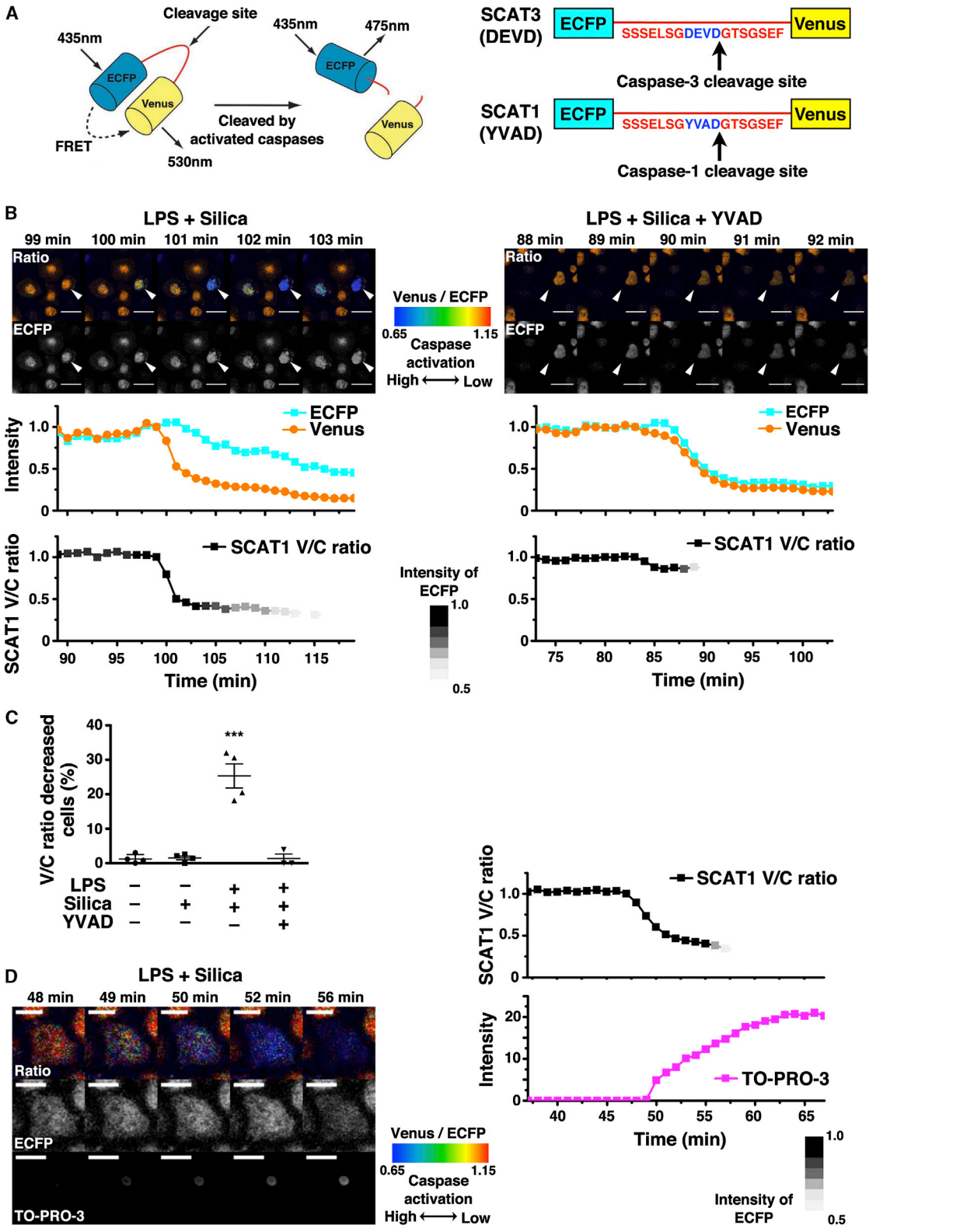

(legend on next page)

in PMΦs exhibited only two patterns: no decrease or dramatic decrease.

Real-Time Detection of Caspase-1 Activation via AIM2 and NLRC4 Inflammasomes

Next, we determined whether SCAT1 detects caspase-1 activation via two other types of inflammasomes, AIM2 and NLRC4, in addition to activation by the NLRP3 inflammasome. The AIM2 inflammasome is activated by poly(dA:dT) transfection with or without LPS priming (Fernandes-Alnemri et al., 2009; Hornung et al., 2009). The SCAT1 V/C ratio dramatically decreased in some PMΦs after poly(dA:dT) transfection in a manner independent of LPS priming (Figures 2A, 2B, and S3A–S3C; Movie S2). This decrease was abolished when the caspase-1 inhibitor was added to SCAT1$^+$ PMΦs or SCAT1$^+$ caspase-1/11-deficient PMΦs (Figures 2A, 2B, and S3B–S3D; Movie S2) (Kayagaki et al., 2011; Kuida et al., 1995). Regardless of the presence or absence of caspase-1 activity, cell death occurred, which was indicated by the disappearance of SCAT1 fluorescence (shown as a loss of ECFP intensity in the SCAT1 V/C ratio graphs in Figures 1B, 1D, 2A, 2C, S2C, S3A, S4A, and S4B).

The NLRC4 inflammasome is activated by pathogenic proteins derived from various bacteria, including *Salmonella* serotype Typhimurium, *Legionella pneumophila*, and *Pseudomonas aeruginosa* (Franchi et al., 2012). SCAT1 V/C ratios rapidly decreased after infection with *S.* Typhimurium SL1344 (Figure 2C), but not after infection with *S.* TyphimuriumΔ invGsseD (a strain that exhibits little capability to induce inflammasomes) or when caspase-1 was inhibited (Figures S4A and S4B; Movie S3). Taken together, these data indicate that SCAT1 detects caspase-1 activation and subsequent cell death that occur via activation of the AIM2, NLRC4, and NLRP3 inflammasomes.

Nearly Identical Kinetics of Caspase-1 Activation and the Resulting Inflammatory Cell Death in Response to Distinct Stimuli

The results of our SCAT1 imaging suggested that caspase-1 activation is a digital, all-or-none response. To quantify and characterize the caspase-1 activation further, we conducted kinetic analyses of caspase-1 activation at the single-cell level. We first investigated whether the kinetics of caspase-1 activation varied in relation to the distinct types of inflammasomes at the single-cell level. The AIM2, NLRP3, and NRLC4 inflammasomes stimulated similar time courses of change in the SCAT1 V/C ratio in response to poly(dA:dT), silica, and *S.* Typhimurium (Figure 3A).

Next, we examined whether varying the stimulus intensity affects the dynamics of caspase-1 activation at the single-cell level. We used poly(dA:dT) as a model stimulus because it does not require LPS priming, which may induce unexpected disparities in cellular competence to stimulus. We transfected poly(dA:dT) into PMΦs at five concentrations and measured the kinetics of caspase-1 activation. The results revealed that the kinetics of caspase-1 activation (change in the relative SCAT1 V/C ratio over time) was similar across all stimulus intensities (Figure 3B). However, stimulus intensity affected the number of PMΦs that contained activated caspase-1 and subsequently underwent cell death, and this number increased in a dose-dependent manner (Figure 3C). Moreover, IL-1β production measured using ELISA, a bulk assay, exhibited a similar trend in the number of PMΦs that contained activated caspase-1 and underwent cell death under LPS-primed conditions (Figure 3D), as previously reported (Nyström et al., 2013).

These results further indicated that caspase-1 is activated in a digital manner. Varying the stimulus intensity or the inflammasome type did not affect the kinetics of caspase-1 activation at the single-cell level; however, at the population level, it influenced the frequency of cell death as a result of inflammasome activation.

Dying PMΦs Containing Activated Caspase-1 as the Main Source of Secreted IL-1β

Our results raised the possibility that PMΦs undergoing cell death immediately after caspase-1 activation are the main source of secreted IL-1β. Although this possibility has long been considered, single-cell studies are required to test the possibility directly and precisely, and few such investigations have been conducted because of technical limitations (Perregaux and Gabel, 1994). Our SCAT1 system allowed us to perform concurrent live imaging of caspase-1 activation, cell death, and IL-1β secretion and combine it with quantitative monitoring of IL-1β secretion in real time at single-cell resolution using a method that we recently developed (Shirasaki et al., 2014). SCAT1$^+$ PMΦs seeded on a microwell device were used to measure caspase-1 activation and IL-1β secretion at single-cell resolution on total internal reflection fluorescent microscopy. After stimulation with poly(dA:dT), the cellular activity of caspase-1 and subsequent IL-1β release from single cells were successfully detected (Figure 4A; Movie S4). IL-1β was secreted in massive amounts immediately after caspase-1 activation, and we therefore called this release an IL-1β burst. Notably, the IL-1β burst coincided with the time of cell death, which was indicated by

Figure 1. Real-Time Detection of Caspase-1 Activation through the NLRP3 Inflammasome with SCAT1, a Genetically Encoded Probe for Monitoring Caspase-1 Activation

(A) Schematic representation of SCAT1, a fluorescence resonance energy transfer biosensor developed for monitoring caspases activation. Right, linker sequences of SCAT3 (caspase-3 cleavage site DEVD) and SCAT1 (caspase-1 cleavage site YVAD).

(B and C) Live-imaging analysis of SCAT1$^+$ macrophages (PMΦs) primed with lipopolysaccharide (LPS) and stimulated with silica. Top, SCAT1 Venus/ECFP (V/C) ratio images of PMΦs treated with LPS (1 μg/ml) + silica (0.5 mg/ml) and LPS (1 μg/ml) + silica (0.5 mg/ml) + YVAD (50 μM). Bottom, time course of relative intensities of ECFP and Venus or SCAT1 V/C ratio changes of PMΦs indicated by arrowheads. The percentages of cells in a field that showed reduced SCAT1 V/C ratio are presented as means and standard deviation (SD) (C). YVAD: z-YVAD-fmk, caspase-1 inhibitor. Scale bar, 50 μm; arrowhead: representative cell. Data are representative of three or more independent experiments in (B); $n > 4$ under each condition, and $^{***}p < 0.001$ (one-way analysis of variance [ANOVA]) in (C).

(D) Live-imaging analysis of TO-PRO-3 staining of SCAT1$^+$ PMΦs under the LPS + silica stimulation condition. Left, time-lapse images of SCAT1 V/C ratio, ECFP, and TO-PRO-3 uptake. Right, time-course of SCAT1 V/C-ratio change and TO-PRO-3 uptake in the PMΦ. Scale bar, 50 μm. Data are representative of three independent experiments.

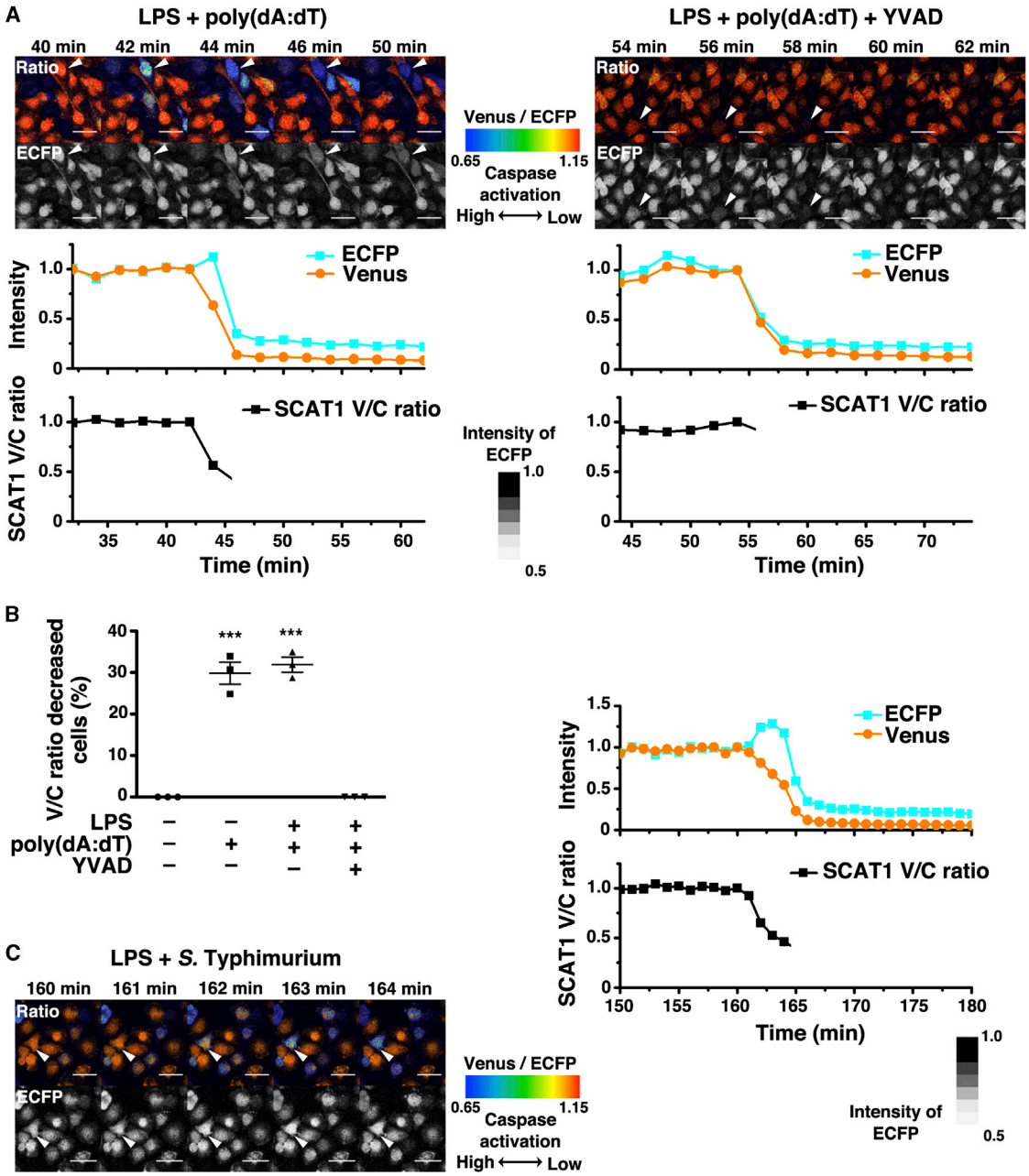

Figure 2. Real-Time Detection of Caspase-1 Activation through the AIM2 and NLRC4 Inflammasomes

(A and B) Live-imaging analysis of SCAT1$^+$ PMΦs under AIM2 inflammasome activation. Top, SCAT1 V/C ratio changes of SCAT1$^+$ PMΦs transfected with LPS (1 μg/ml) + poly(dA:dT) (1 μg/ml) and LPS (1 μg/ml) + poly(dA:dT) (1 μg/ml) + YVAD (50 μM). Bottom, time course of changes in the relative intensity of ECFP and Venus or SCAT1 V/C ratios of PMΦs indicated by arrowheads. The percentages of cells in a field that showed a reduction in the SCAT1 V/C ratio are presented as means and SD (B). Scale bar, 50 μm; arrowhead: representative cell. Data are representative of three independent experiments in (A); n > 3 under each condition, ***p < 0.001 (one-way ANOVA) in (B).

(C) Live-imaging analysis of SCAT1$^+$ PMΦs under NLRC4 activation. Left, SCAT1 V/C ratio images of PMΦs primed with LPS (1 μg/ml) and infected with *Salmonella* Typhimurium (MOI 20). Right, time course of changes in the relative intensities of ECFP and Venus or SCAT1 V/C ratios of the PMΦs indicated by arrowheads. Scale bar, 50 μm; arrowhead: representative cell. Data are representative of three independent experiments.

the disappearance of SCAT1 fluorescence (52 min in Figures 4A and 4B). To investigate whether all the cells that exhibited the IL-1β burst died, we examined the relationship between the IL-1β signal and cell death. Our results indicated that the cells that secreted IL-1β also died and that no surviving cells secreted IL-1β under this condition (Figure 4C). Furthermore, inhibiting caspase-1 activation did not inhibit cell death but prevented IL-1β release (Figure 4C). These results clearly demonstrated

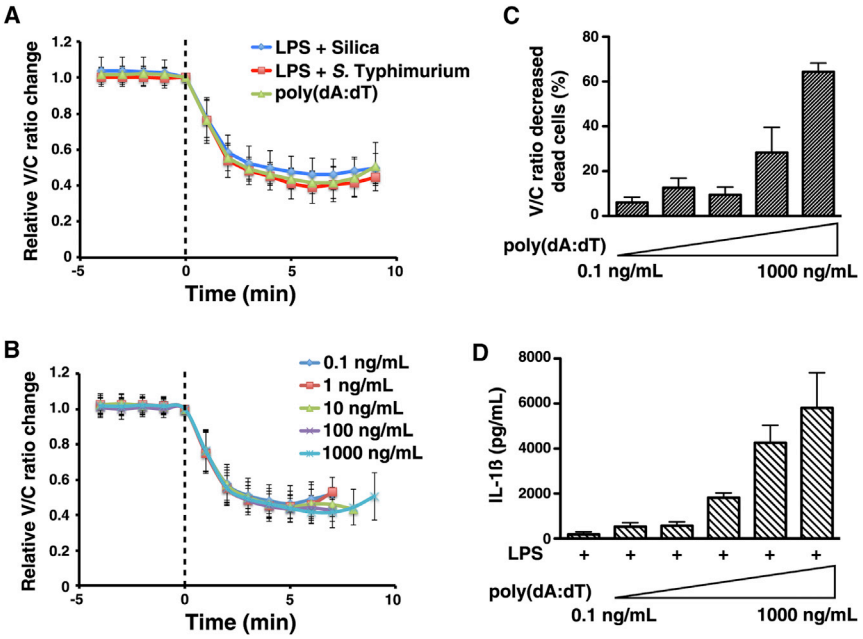

Figure 3. Almost Identical Kinetics of Caspase-1 Activation and Resulting Inflammatory Cell Death Induced by Distinct Stimuli

(A and B) Relative SCAT1 V/C ratio changes before and after caspase-1 activation. PMΦs were stimulated with distinct inflammasome activators (NLRP3: LPS [1 μg/ml] + silica [0.5 mg/ml], NLRC4: LPS [1 μg/ml] + *S.* Typhimurium [MOI 20], and AIM2: poly[dA:dT] [1 μg/ml]) (A) or transfected with poly(dA:dT) (0.1, 1, 10, 100, and 1,000 ng/ml) (B) and then examined live for 4 hr. Numbers of cells (n) used for quantifying SCAT1 V/C ratios under various conditions were (A) 32 for LPS + silica, 26 for LPS + *S.* Typhimurium, and 115 for poly(dA:dT). For poly(dA:dT) in (B), n = 42 (0.1 ng/ml), 78 (1 ng/ml), 64 (10 ng/ml), 88 (100 ng/ml), and 119 (1,000 ng/ml). x axis, time (min). Data were collected from two or more independent experiments and are presented as mean and SD.

(C) Percentages of PMΦs that contained activated caspase-1 and died, as determined based on the loss of fluorescence in all cells examined under the microscope. PMΦs were transfected with poly(dA:dT) (0.1, 1, 10, 100, and 1,000 ng/ml) and imaged live for 3 hr. Data were collected from four independent experiments and are presented as mean and SD.

(D) ELISA performed on interleukin (IL)-1β that was secreted into cell culture supernatants from SCAT1$^+$ PMΦs. The PMΦs were primed with LPS (1 μg/ml) for 4 hr and transfected with poly(dA:dT) (0.1, 1, 10, 100, 1000 ng/ml) for 3 hr. Data were collected from four independent experiments and are presented as mean and SD.

that inflammasome-mediated digital activation of caspase-1 couples the IL-1β burst with cell death and that dying cells containing activated caspase-1 are the main source of secreted IL-1β in PMΦ populations.

DISCUSSION

This study, which used a probe designed to detect caspase-1 activation, showed that caspase-1 activation is an all-or-none response at the single-cell level in PMΦs. It also demonstrated that the kinetics of caspase-1 is essentially the same irrespective of the intensity or types of stimulus. The output of caspase-1 activation is a burst of IL-1β release, which also occurs in an all-or-none manner as a consequence of digital activation of caspase-1. However, the mechanisms underlying these digital, all-or-none responses remain unclear. The assembly of large oligomeric signalosomes containing members of the Toll-like receptor interleukin-1 receptor superfamily has been suggested to be a structural basis for a digital all-or-none response (Ferrao et al., 2012; Wu, 2013). As well, such higher-order signalosomes have recently been reported to exist in inflammasomes (Lu et al., 2014), which may be the mechanism that dictates the digital activation of caspase-1.

Caspase-1 activation has long been considered to induce IL-1β secretion and cell death, and IL-1β secretion is correlated with cell death (Brough and Rothwell, 2007; Hogquist et al., 1991; Nyström et al., 2013). However, whether individual cells that contain activated caspase-1 secrete IL-1β and die has remained unclear because the investigative methods available to date have been bulk assays, which cannot address these questions. Recently, two biosensors that monitor caspase-1 and inflammasome activation were reported: a bioluminescence resonance energy transfer sensor to detect pro-IL-1β processing and a sensor fusion protein of luciferase and pro-IL-1β (Bartok et al., 2013; Compan et al., 2012). Such luminescence-based probes are superior to fluorescent probes in that they allow examination of bulk activity in cell populations or at the tissue level; however, the cellular resolution and sensitivity of these probes are insufficient for single-cell analysis within tissues. Furthermore, these sensors appear inadequate from a time-resolution standpoint for determining the kinetics of rapid caspase-1 activation within a single cell. By comparison, the indicator we developed, SCAT1, enables visualization of caspase-1 activation and measurement of its kinetics at high temporal resolution on the single-cell level. Although we do not exclude the possibility that our SCAT1 and IL-1β imaging are insensitive to weak or local activations of caspase-1 and very low amounts of IL-1β secretion, previous bulk assays including western blotting and ELISA are less sensitive than our single-cell imaging system and almost impossible to use to test this possibility. Addressing these issues requires further technical developments.

Elevated local or systemic IL-1β release caused by compromised inflammasome activation is associated with various chronic inflammatory diseases such as cryopyrin-associated periodic syndrome, metabolic disorders, and carcinogenesis in human and mouse models (Wen et al., 2012; Zitvogel et al., 2012). Recently, mutations in an NLRP3 protein associated with cryopyrin-associated periodic syndrome were shown to induce necrotic cell death, which in turn leads to neutrophilic inflammation (Satoh et al., 2013). Our study clearly demonstrates that dying MΦs containing activated caspase-1 exhibit IL-1β bursts. Thus, cells located near such MΦs would receive a maximal level

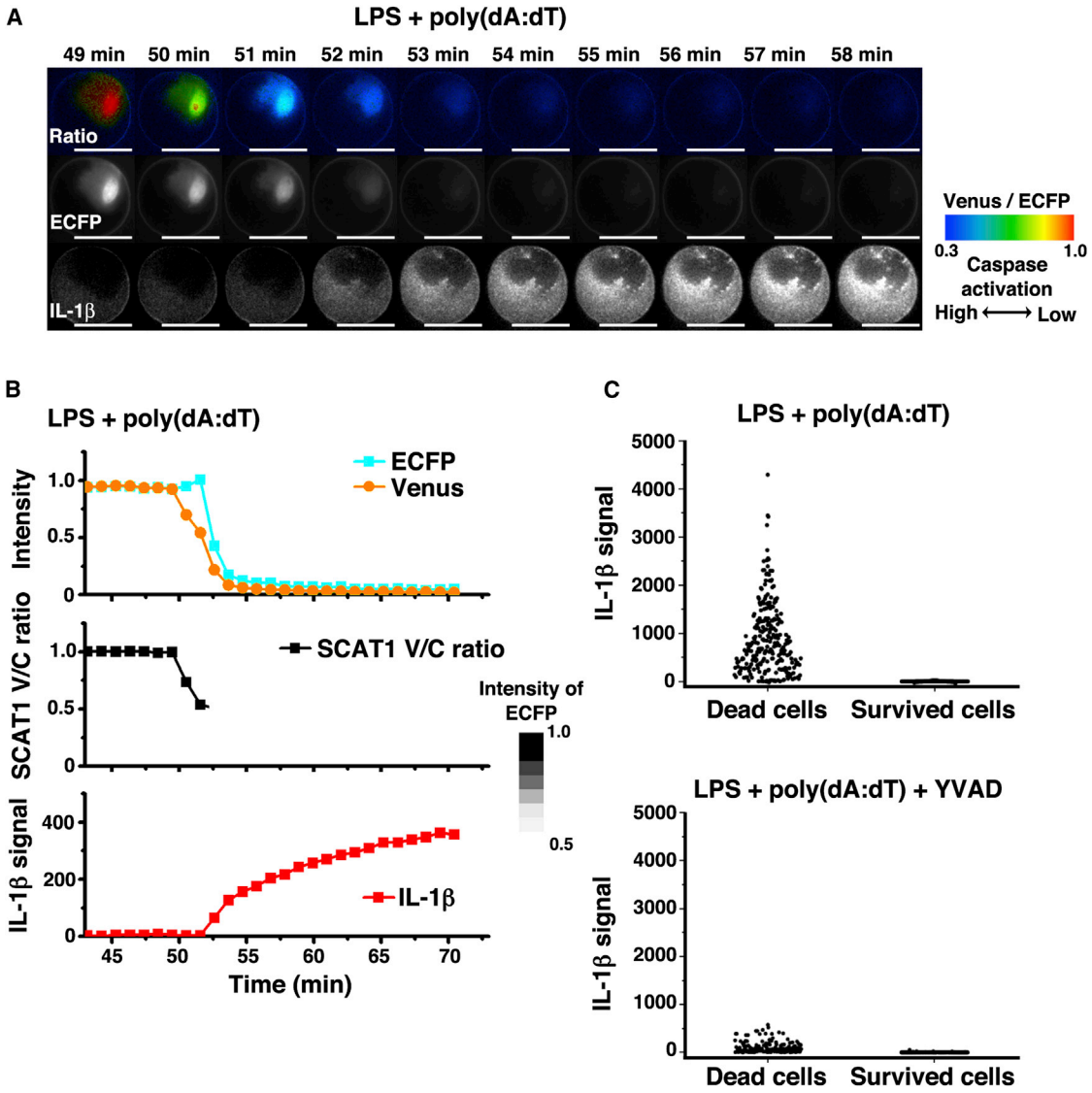

Figure 4. Dying PMΦs Containing Activated Caspase-1 as the Main Source of Secreted IL-1β

(A and B) Simultaneous live imaging of SCAT1 V/C-ratio changes and IL-1β secretion in SCAT1$^+$ PMΦs primed using LPS (1 μg/ml) and stimulated with poly(dA:dT) (1 μg/ml). (A) The montage shows time-dependent changes in the intensities of ECFP (the middle row), SCAT1 V/C ratios (the top row), and IL-1β secretion (the bottom row). (B) The time course of changes in the intensities of ECFP and Venus, SCAT1 V/C ratios, and IL-1β secretion in a representative cell, as in (A). Scale bar, 50 μm.

(C) Dot-plot representation of the signal intensity of IL-1β secreted from single cells, classified according to cell viability in the absence and presence of treatment with the caspase-1 inhibitor YVAD. LPS-primed SCAT1$^+$ PMΦs were introduced into a microwell array with a fluorescent detection antibody and stimulated with poly(dA:dT). After incubation for 4 hr, all microwells were scanned to detect the signals of IL-1β secretion and the SCAT1 probe. Cell viability was determined based on the intensity of SCAT1.

of IL-1β locally, even when a low level of circulating IL-1β is detected systemically. This scenario is highly likely to occur under chronic disease conditions. If the local cells receiving the burst-released IL-1β exhibit oncogenic potential, strong stimulation by high levels of IL-1β could trigger cellular transformation under conditions of chronic inflammation. Studies of inflammatory cell death and local bursts of cytokine release in vivo could offer intriguing and crucial perspectives that will help reveal the mechanisms underlying chronic inflammatory diseases. Applying SCAT1 imaging analysis to various chronic inflammatory disease models in vivo is challenging but would enhance our understanding of the involvement of local and continuous inflammatory cell death in the pathology of these diseases.

EXPERIMENTAL PROCEDURES

Live Imaging of Peritoneal MΦ Cultures

Live imaging was conducted using an inverted confocal microscope (TCS SP5; Leica) equipped with a galvo stage and a resonant scanner designed for fast scanning using an HC PL APO 20×/0.70 CS dry objective (Leica).

During imaging, dishes of cells were placed in a humidified cell-culture incubator and continuously supplied with 5% CO_2/air at 37°C (Tokai Hit Company). ECFP was excited using a 442 nm diode laser (10%–25% power), and the emissions of ECFP and Venus (FRET) were detected simultaneously using two detectors (Leica HyD) and a resonant scanner (8,000 Hz; Leica). Propidium iodide and TO-PRO-3 were excited using 561 and 633 nm diode lasers (15% power), respectively. Images (512 × 512 pixels) were acquired at intervals of 1–2 min, and the z slices obtained were 4 μm thick (total of 9–12 slices/time point), depending on the experiment. To inhibit caspase-1 pharmacologically, we used z-YVAD-fmk (50 μM final concentration; 1/1,000 dilution of a 50 mM stock prepared in dimethylsulfoxide).

PMΦs were plated on four-well glass-bottom dishes (Greiner Bio-One) and primed using LPS (1 μg/ml) or PBS for 4–12 hr before stimulation. All live-imaging analyses were initiated after stimulating inflammasomes by using this procedure, and live images were acquired for 3–4 hr under all conditions tested.

SUPPLEMENTAL INFORMATION

Supplemental Information includes Supplemental Experimental Procedures, four figures, and four movies and can be found with this article online at http://dx.doi.org/10.1016/j.celrep.2014.07.012.

AUTHOR CONTRIBUTIONS

T.L., Y.Y., and M.M. designed the study; T.L., Y.S., K.S., and Y.Y. performed most of the experiments and data analysis; Y.S. and M.Y. performed the single-cell live imaging of cytokine secretion and data analysis; K.H., T.K., K.T., T.S., E.K., and O.O. provided essential advice and resources; and T.L., Y.Y., and M.M. prepared the manuscript.

ACKNOWLEDGMENTS

We are grateful to K. Kuida (Millennium: The Takeda Oncology Company), R. Uchiyama, and H. Tsutsui (Hyogo College of Medicine, Japan) for providing caspase-1/11-deficient mice, M. Okabe (Osaka University) for providing CAG-Cre mice (Riken BRC), and Y. Sasaki (Kyoto University) for providing the Rosa26-CAG-STOP targeting vector. We thank the University of Tokyo and Leica Microsystems Imaging Center for the imaging analysis. We also thank N. Kambe (Chiba University), T. Chihara, and all the members of the M.M. laboratory for the helpful discussions and comments and M. Sasaki, K. Tomioka, Y. Fujioka, T. Takahashi, and Y. Watanabe for experimental assistance. This work was supported by grants to M.M. and Y.Y. from the Ministry of Education, Culture, Sports, Science and Technology in Japan, the Japan Society for the Promotion of Science, and the Japan Science and Technology Agency.

Received: December 27, 2013
Revised: May 26, 2014
Accepted: July 13, 2014
Published: August 7, 2014

REFERENCES

Aoki, K., Kamioka, Y., and Matsuda, M. (2013). Fluorescence resonance energy transfer imaging of cell signaling from in vitro to in vivo: basis of biosensor construction, live imaging, and image processing. Dev. Growth Differ. *55*, 515–522.

Bartok, E., Bauernfeind, F., Khaminets, M.G., Jakobs, C., Monks, B., Fitzgerald, K.A., Latz, E., and Hornung, V. (2013). iGLuc: a luciferase-based inflammasome and protease activity reporter. Nat. Methods *10*, 147–154.

Brough, D., and Rothwell, N.J. (2007). Caspase-1-dependent processing of pro-interleukin-1beta is cytosolic and precedes cell death. J. Cell Sci. *120*, 772–781.

Broz, P., von Moltke, J., Jones, J.W., Vance, R.E., and Monack, D.M. (2010). Differential requirement for Caspase-1 autoproteolysis in pathogen-induced cell death and cytokine processing. Cell Host Microbe *8*, 471–483.

Compan, V., Baroja-Mazo, A., Bragg, L., Verkhratsky, A., Perroy, J., and Pelegrin, P. (2012). A genetically encoded IL-1β bioluminescence resonance energy transfer sensor to monitor inflammasome activity. J. Immunol. *189*, 2131–2137.

Denes, A., Lopez-Castejon, G., and Brough, D. (2012). Caspase-1: is IL-1 just the tip of the ICEberg? Cell Death Dis. *3*, e338.

Fernandes-Alnemri, T., Yu, J.W., Datta, P., Wu, J., and Alnemri, E.S. (2009). AIM2 activates the inflammasome and cell death in response to cytoplasmic DNA. Nature *458*, 509–513.

Ferrao, R., Li, J., Bergamin, E., and Wu, H. (2012). Structural insights into the assembly of large oligomeric signalosomes in the Toll-like receptor-interleukin-1 receptor superfamily. Sci. Signal. *5*, re3.

Fink, S.L., and Cookson, B.T. (2005). Apoptosis, pyroptosis, and necrosis: mechanistic description of dead and dying eukaryotic cells. Infect. Immun. *73*, 1907–1916.

Franchi, L., Muñoz-Planillo, R., and Núñez, G. (2012). Sensing and reacting to microbes through the inflammasomes. Nat. Immunol. *13*, 325–332.

Hogquist, K.A., Nett, M.A., Unanue, E.R., and Chaplin, D.D. (1991). Interleukin 1 is processed and released during apoptosis. Proc. Natl. Acad. Sci. USA *88*, 8485–8489.

Hornung, V., Ablasser, A., Charrel-Dennis, M., Bauernfeind, F., Horvath, G., Caffrey, D.R., Latz, E., and Fitzgerald, K.A. (2009). AIM2 recognizes cytosolic dsDNA and forms a caspase-1-activating inflammasome with ASC. Nature *458*, 514–518.

Kayagaki, N., Warming, S., Lamkanfi, M., Vande Walle, L., Louie, S., Dong, J., Newton, K., Qu, Y., Liu, J., Heldens, S., et al. (2011). Non-canonical inflammasome activation targets caspase-11. Nature *479*, 117–121.

Keller, M., Rüegg, A., Werner, S., and Beer, H.D. (2008). Active caspase-1 is a regulator of unconventional protein secretion. Cell *132*, 818–831.

Kuida, K., Lippke, J.A., Ku, G., Harding, M.W., Livingston, D.J., Su, M.S., and Flavell, R.A. (1995). Altered cytokine export and apoptosis in mice deficient in interleukin-1 beta converting enzyme. Science *267*, 2000–2003.

Kuranaga, E., Matsunuma, T., Kanuka, H., Takemoto, K., Koto, A., Kimura, K., and Miura, M. (2011). Apoptosis controls the speed of looping morphogenesis in Drosophila male terminalia. Development *138*, 1493–1499.

Latz, E., Xiao, T.S., and Stutz, A. (2013). Activation and regulation of the inflammasomes. Nat. Rev. Immunol. *13*, 397–411.

Lu, A., Magupalli, V.G., Ruan, J., Yin, Q., Atianand, M.K., Vos, M.R., Schröder, G.F., Fitzgerald, K.A., Wu, H., and Egelman, E.H. (2014). Unified polymerization mechanism for the assembly of ASC-dependent inflammasomes. Cell *156*, 1193–1206.

Martinon, F., Burns, K., and Tschopp, J. (2002). The inflammasome: a molecular platform triggering activation of inflammatory caspases and processing of proIL-beta. Mol. Cell *10*, 417–426.

Miao, E.A., Leaf, I.A., Treuting, P.M., Mao, D.P., Dors, M., Sarkar, A., Warren, S.E., Wewers, M.D., and Aderem, A. (2010). Caspase-1-induced pyroptosis is an innate immune effector mechanism against intracellular bacteria. Nat. Immunol. *11*, 1136–1142.

Miura, M., Zhu, H., Rotello, R., Hartwieg, E.A., and Yuan, J. (1993). Induction of apoptosis in fibroblasts by IL-1 beta-converting enzyme, a mammalian homolog of the C. elegans cell death gene ced-3. Cell *75*, 653–660.

Mosser, D.M., and Edwards, J.P. (2008). Exploring the full spectrum of macrophage activation. Nat. Rev. Immunol. *8*, 958–969.

Nakajima, Y., Kuranaga, E., Sugimura, K., Miyawaki, A., and Miura, M. (2011). Nonautonomous apoptosis is triggered by local cell cycle progression during epithelial replacement in Drosophila. Mol. Cell. Biol. *31*, 2499–2512.

Nyström, S., Antoine, D.J., Lundbäck, P., Lock, J.G., Nita, A.F., Högstrand, K., Grandien, A., Erlandsson-Harris, H., Andersson, U., and Applequist, S.E. (2013). TLR activation regulates damage-associated molecular pattern isoforms released during pyroptosis. EMBO J. *32*, 86–99.

Perregaux, D., and Gabel, C.A. (1994). Interleukin-1 beta maturation and release in response to ATP and nigericin. Evidence that potassium depletion

mediated by these agents is a necessary and common feature of their activity. J. Biol. Chem. *269*, 15195–15203.

Pierini, R., Juruj, C., Perret, M., Jones, C.L., Mangeot, P., Weiss, D.S., and Henry, T. (2012). AIM2/ASC triggers caspase-8-dependent apoptosis in Francisella-infected caspase-1-deficient macrophages. Cell Death Differ. *19*, 1709–1721.

Rathinam, V.A., Vanaja, S.K., and Fitzgerald, K.A. (2012). Regulation of inflammasome signaling. Nat. Immunol. *13*, 333–342.

Satoh, T., Kambe, N., and Matsue, H. (2013). NLRP3 activation induces ASC-dependent programmed necrotic cell death, which leads to neutrophilic inflammation. Cell Death Dis. *4*, e644.

Schroder, K., and Tschopp, J. (2010). The inflammasomes. Cell *140*, 821–832.

Shirasaki, Y., Yamagishi, M., Suzuki, N., Izawa, K., Nakahara, A., Mizuno, J., Shoji, S., Heike, T., Harada, Y., Nishikomori, R., and Ohara, O. (2014). Real-time single-cell imaging of protein secretion. Sci Rep *4*, 4736.

Takemoto, K., Nagai, T., Miyawaki, A., and Miura, M. (2003). Spatio-temporal activation of caspase revealed by indicator that is insensitive to environmental effects. J. Cell Biol. *160*, 235–243.

Takemoto, K., Kuranaga, E., Tonoki, A., Nagai, T., Miyawaki, A., and Miura, M. (2007). Local initiation of caspase activation in Drosophila salivary gland programmed cell death in vivo. Proc. Natl. Acad. Sci. USA *104*, 13367–13372.

Tay, S., Hughey, J.J., Lee, T.K., Lipniacki, T., Quake, S.R., and Covert, M.W. (2010). Single-cell NF-kappaB dynamics reveal digital activation and analogue information processing. Nature *466*, 267–271.

Walsh, J.G., Logue, S.E., Lüthi, A.U., and Martin, S.J. (2011). Caspase-1 promiscuity is counterbalanced by rapid inactivation of processed enzyme. J. Biol. Chem. *286*, 32513–32524.

Wen, H., Ting, J.P., and O'Neill, L.A. (2012). A role for the NLRP3 inflammasome in metabolic diseases—did Warburg miss inflammation? Nat. Immunol. *13*, 352–357.

Wu, H. (2013). Higher-order assemblies in a new paradigm of signal transduction. Cell *153*, 287–292.

Yamaguchi, Y., Shinotsuka, N., Nonomura, K., Takemoto, K., Kuida, K., Yosida, H., and Miura, M. (2011). Live imaging of apoptosis in a novel transgenic mouse highlights its role in neural tube closure. J. Cell Biol. *195*, 1047–1060.

Zitvogel, L., Kepp, O., Galluzzi, L., and Kroemer, G. (2012). Inflammasomes in carcinogenesis and anticancer immune responses. Nat. Immunol. *13*, 343–351.